Calicheamicin Antibody–Drug Conjugates with Improved Properties

Breanna S. Vollmar[1], Chris Frantz[1], Melissa M. Schutten[1], Fiona Zhong[1], Geoffrey del Rosario[1], Mary Ann T. Go[1], Shang-Fan Yu[1], Douglas D. Leipold[1], Amrita V. Kamath[1], Carl Ng[1], Keyang Xu[1], Josefa dela Cruz-Chuh[1], Katherine R. Kozak[1], Jinhua Chen[2], Zijin Xu[2], John Wai[2], Pragya Adhikari[1], Hans K. Erickson[1], Peter S. Dragovich[1], Andrew G. Polson[1], and Thomas H. Pillow[1]

ABSTRACT

Calicheamicin antibody–drug conjugates (ADCs) are effective therapeutics for leukemias with two recently approved in the United States: Mylotarg (gemtuzumab ozogamicin) targeting CD33 for acute myeloid leukemia and Besponsa (inotuzumab ozogamicin) targeting CD22 for acute lymphocytic leukemia. Both of these calicheamicin ADCs are heterogeneous, aggregation-prone, and have a shortened half-life due to the instability of the acid-sensitive hydrazone linker in circulation. We hypothesized that we could improve upon the heterogeneity, aggregation, and circulation stability of calicheamicin ADCs by directly attaching the thiol of a reduced calicheamicin to an engineered cysteine on the antibody via a disulfide bond to generate a linkerless and traceless conjugate. We report herein that the resulting homogeneous conjugates possess minimal aggregation and display high *in vivo* stability with 50% of the drug remaining conjugated to the antibody after 21 days. Furthermore, these calicheamicin ADCs are highly efficacious in mouse models of both solid tumor ($HER2^+$ breast cancer) and hematologic malignancies ($CD22^+$ non-Hodgkin lymphoma). Safety studies in rats with this novel calicheamicin ADC revealed an increased tolerability compared with that reported for Mylotarg. Overall, we demonstrate that applying novel linker chemistry with site-specific conjugation affords an improved, next-generation calicheamicin ADC.

Introduction

Antibody–drug conjugates (ADCs) represent an ever-growing class of targeted therapeutics with more than 60 candidates in clinical evaluation for various oncological indications (1). ADCs are composed of a cytotoxic payload conjugated to a tumor-targeting antibody. Of the nine ADCs that are currently approved, two are conjugated to calicheamicin, a potent drug that causes DNA damage (Mylotarg and Besponsa), five consist of tubulin-targeting agents, auristatin and maytansine (Blenrep, Padcev, Polivy, Adcetris, Kadcyla) and most recently, two utilize topoisomerase inhibitors (Trodelvy, Enhertu). Calicheamicin-based ADCs (cal-ADCs) represent the earliest class of ADCs marketed for use in humans with the approval of Mylotarg for acute myeloid leukemia (AML) in 2000 (2). Mylotarg was voluntarily withdrawn from the market in 2010 due to safety concerns identified in a post approval study that demonstrated increased mortality and incidence of hepatic veno-occlusive disease associated with Mylotarg (3). However, Mylotarg was recently reapproved for AML with new data from follow-up clinical trials that demonstrated efficacy with an acceptable safety profile utilizing a dose fractionation schedule and treating only patients with newly diagnosed AML, rather than after first relapse (4–6). A second cal-ADC (Besponsa) was also approved in 2017 for acute lymphocytic leukemia (7). With the recent approval of two cal-ADCs, there is renewed interest in evaluating this potent payload class utilizing recent understandings and technological advancements in ADCs.

Apart from the target antigen, Mylotarg and Besponsa use the same antibody isotype, conjugation chemistry, linker design, and calicheamicin derivative. Mylotarg and Besponsa are composed of an IgG4 humanized antibody, targeting CD33 and CD22, respectively, conjugated to calicheamicin via an acid-labile linker (**Fig. 1**; refs. 8, 9). Both are considered first-generation ADCs because they utilize N-hydroxysuccinimide chemistry to conjugate calicheamicin to lysines on the antibody surface yielding a heterogeneous mixture with different drug-to-antibody ratios (DARs). The linker between the antibody and the payload consists of three components, an acid-labile hydrazone followed by a dimethyl disulfide separated by an aromatic spacer termed AcButDMH linker (**Fig. 1A**; ref. 8). The acid cleavable hydrazone is designed to be stable in the neutral pH conditions encountered during circulation, but will readily undergo hydrolysis under the acidic conditions of the lysosome inside of cells. The dimethyl disulfide preserves the natural disulfide trigger mechanism of calicheamicin, while the added sterics from the methyl groups are thought to protect the disulfide during circulation (10). Once the ADC is internalized and degraded in the lysosome, the potent calicheamicin derivative, N-acetyl-γ-calicheamicin (NAc-calicheamicin), is then activated by reduction of the dimethyl disulfide trigger in the cytosol to form the potent enediyne diradical capable of inducing DNA strand breaks (11). Notably, all of the cal-ADCs that have undergone preclinical [Lewis-y (12), 5T4 (13, 14)] and clinical development [CD33 (8), CD22 (15), EFNA-4 (16, 17)] have utilized this AcButDMH linker (**Fig. 1A**) with the exception of CMB-401 (18), which contained an uncleavable linker.

Despite the extensive preclinical studies that led to the optimized AcButDMH linker for cal-ADCs (8, 18–20), recent studies have suggested that the instability of hydrazone linkers is a potential

[1]Genentech, Inc., South San Francisco, California. [2]WuXi AppTec Co., Ltd, Shanghai, China.

Note: Supplementary data for this article are available at Molecular Cancer Therapeutics Online (http://mct.aacrjournals.org/).

Corresponding Author: Thomas H. Pillow, Research and Early Development, Genentech, Inc., South San Francisco, CA 94080. Phone: 650-225-1652; Fax: 650-467-5155; E-mail: thomashp@gene.com

Mol Cancer Ther 2021;20:1112–20

doi: 10.1158/1535-7163.MCT-20-0035

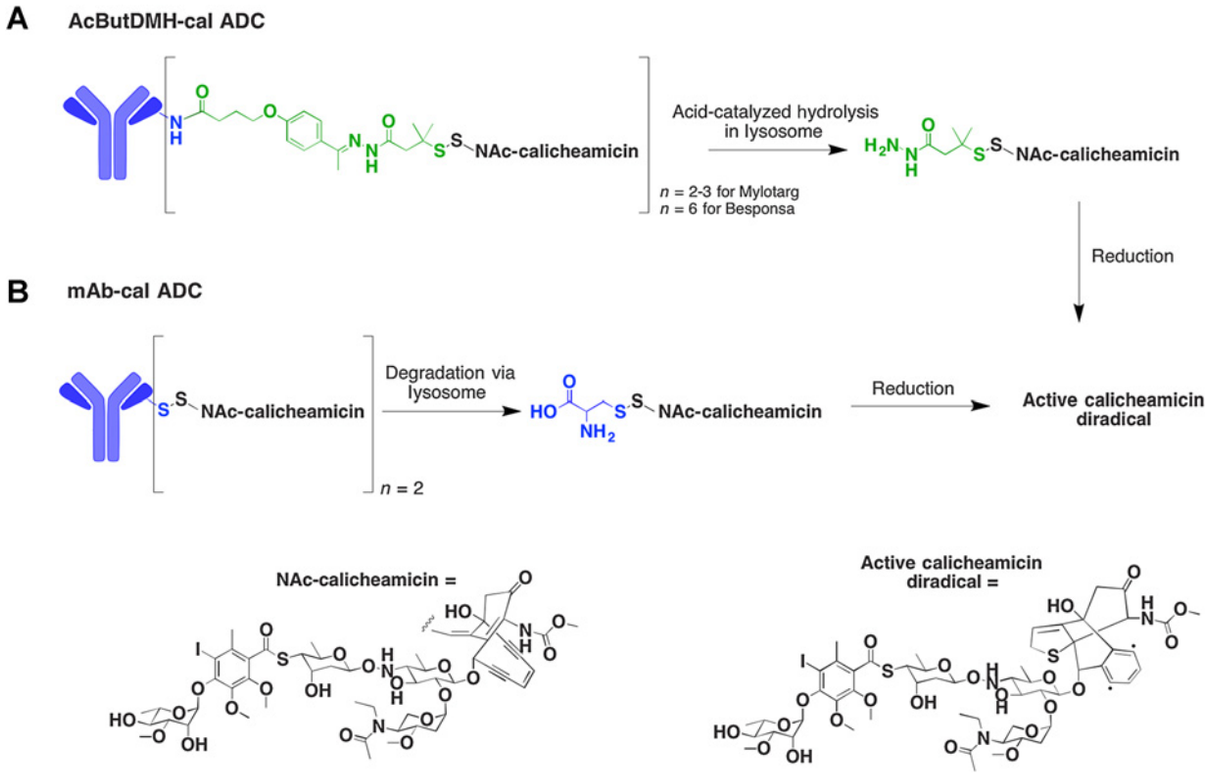

Figure 1.

AcButDMH and linkerless calicheamicin ADCs. **A,** Besponsa and Mylotarg both utilize the AcButDMH linker, such that the active payload is released upon hydrolysis followed by reduction of the disulfide. **B,** Linkerless calicheamicin ADC (mAb-cal ADC) is connected through a disulfide formed between the engineered cysteine sulfur of the antibody and the sulfur of reduced NAc-calicheamicin. The active diradical payload is generated upon reduction of the disulfide.

liability. Comparison of the widely used valine-citrulline protease cleavable linker to an acid-labile hydrazone linker, similar to AcButDMH, has shown that the hydrazone is considerably less stable in mouse and human plasma (21). Furthermore, *in vitro* cytotoxicity assays show a loss of target-specific potency under continuous exposure of the ADC suggesting premature hydrolysis of the hydrazone and release of the active species in the media (21). Pharmacokinetic studies describing the stability of Mylotarg and Besponsa in mice confirm that the AcButDMH-cal ADCs have conjugated drug half-lives of approximately 47 and 29 hours, respectively (22). From the clinical pharmacokinetic data available for Mylotarg and Besponsa, it is clear that the short half-life observed preclinically for the cal-ADCs has translated to short half-life of the conjugated ADCs in humans. The human half-lives of 67 hours (2) and 17 hours (23), respectively, suggests nonspecific release of the potent cytotoxin in circulation (24).

We hypothesized that we could improve upon these first-generation cal-ADCs by utilizing novel linker and conjugation chemistry coupled with antibody engineering. First of all, we proposed to conjugate calicheamicin to a specific site on the antibody as this has been demonstrated with other drugs to increase efficacy and decrease toxicity compared with conjugation chemistries yielding heterogeneous mixtures (25). Second, we desired a linker that would stably connect and tracelessly release calicheamicin. Traceless disulfide linkers were initially developed to connect thiol-containing drugs to small proteins, but the stability and release profile was insufficient for effective antibody-mediated delivery (26, 27). Circulation stability of the linker is considered to be a crucial parameter for ADCs, with recent studies showing that specific sites on antibodies can confer stability (28–30) and improvements in linker design can lead to sustained stability in circulation (21, 31, 32). Given the evidence suggesting that the hydrazone linker is weakly stable in circulation, we proposed that we could increase the attachment stability of calicheamicin ADCs by conjugating calicheamicin directly to a precisely selected cysteine on a cysteine-engineered or THIOMAB antibody through a disulfide, affording a traceless and effectively "linkerless" conjugate (**Fig. 1B**).

An advantage of this type of novel linkerless connection over the AcButDMH linker used in all but one of the cal-ADCs developed to date is the potential to improve stability in circulation while simultaneously improving intracellular release. Direct connection of the thiol of calicheamicin via a simple unhindered disulfide was postulated to provide sustained circulation stability via the appropriately selected attachment site, which has been shown previously to stabilize unhindered disulfides (31, 32). This stabilizing effect is then eliminated upon internalization and subsequent degradation of the antibody in the lysosome. Furthermore, this stable yet unhindered disulfide would generate a catabolite more readily reduced compared with the sterically hindered dimethyl disulfide hydrazide calicheamicin catabolite arising from the AcButDMH linker (**Fig. 1**). Here we show that this novel linkerless calicheamicin ADC (abbreviated "mAb-cal" for simplicity) conjugates easily with minimal aggregation, exhibits target-specific cell killing, is efficacious in both solid and liquid tumor models, has sustained circulation stability *in vivo*, and has an increased tolerability in rats compared with that reported for Mylotarg.

Materials and Methods

Synthesis of activated disulfide calicheamicin linker drug

To a solution of *N*-acetyl calicheamicin γ1 (20.0 mg, 0.0100 mmol) and Et_3N (3.59 mg, 0.0400 mmol) in acetonitrile (10 mL) was added 5-nitropyridine-2-thiol (6.64 mg, 0.0400 mmol) at 15°C. The reaction mixture was stirred under N_2 at 15°C for 10 hours. The reaction mixture was diluted with EtOAc (20 mL), washed with water (10 mL × 3), dried over anhydrous sodium sulfate, concentrated, and purified by prep-TLC (7% MeOH in DCM, Rf = 0.5). It was further purified by prep-HPLC (acetonitrile 45%–75%/10 mmol/L NH_4HCO_3 in water) to afford nitropyridyldisulfide calicheamicin (nitroPDS-cal; 4.3 mg, 19%) as a gray solid. HRMS: m/z = 1486.2888 [M+1]+.

Preparation of conjugates

All cysteine-engineered antibodies were expressed and purified as described previously using standard methods (31, 33). mAb-cal ADCs were prepared by mixing the antibody with 3 to 10 molar equivalents of nitroPDS-cal at 50 mmol/L Tris pH 7, Tris pH 8, or Tris pH 8.5 with 10% dimethylformamide final. Conjugation reaction was complete after 3 to 5 hours at ambient temperature and purified to remove unconjugated linker drug using cationic exchange chromatography. mAb-cal ADCs were formulated and analyzed using standard conditions as described previously for other disulfide-linked ADCs (31, 33). All conjugates prepared had DAR values > 1.7, < 5% unconjugated linker drug, < 2% aggregation and endotoxin levels < 0.05 EU/mg antibody.

In vitro cytotoxicity assay

On day 0, suspension cell lines, BJAB and WSU-DLCL2 ($CD22^+$ cells) and Jurkat ($CD22^-$ cells), were seeded at 4,000 cells per well in 40-μL RPMI1640 culture media supplemented with 10% FBS, 2 mmol/L glutamine, 50 μmol/L cystine, and 0.015 g/L L-methionine in 384-well flat clear bottom white polystyrene tissue culture-treated microplates (Corning). Adherent Ly6E-positive cell lines, HCC-1569 × 2 and NCI-H1781, were seeded at 1,500 and 5,000 cells per well, respectively. Suspension cells were treated on day 0 after plating, while adherent cells were incubated overnight in a humidified incubator set at 37°C and maintaining an atmosphere of 5% CO_2 before drug and antibody conjugate treatment. Antibody–drug conjugates, 2 mg/mL in 20 mmol/L histidine acetate, 240 mmol/L sucrose, 0.02% PS20 pH 5.5 buffer, were transferred to cells seeded in 384-well plates using ECHO acoustic liquid handling technology (Labcyte Inc) to create a 10-point dose–response curve in triplicate starting from 20 μg/mL with 1:3 × serial dilution. The antiproliferation activity of the ADCs was determined in an 11-point dose–response study starting from 50 nmol/L down to 0.1 pmol/L in 1:4 fold serial dilutions with final 0.25% DMSO in culture medium. Cells were cultured in a humidified incubator set at 37°C and maintaining an atmosphere of 5% CO_2. On day 4 or day 5, suspension cells or adherent cells, respectively, were equilibrated to room temperature, then 40 μL/well Cell Titer Glo II reagent (Promega) was added, plates shaken for 10 minutes, then incubated for 30 minutes at room temperature in the dark. Luminescence was read using an EnVision 2101 Multilabel Reader (PerkinElmer). Normalized luminescence intensity data were analyzed using Genedata Screener version 15 software, and IC_{50} values were calculated using a four-parameter sigmoidal fit.

In vivo efficacy

All animal studies were performed in compliance with NIH guidelines for the care and use of laboratory animals and were approved by the Institutional Animal Care and Use Committee (IACUC) at Genentech, Inc.

A $CD22^+$ human non-Hodgkin lymphoma cell line WSU-DLCL2 (DSMZ) and a $Ly6E^+$ human breast cancer cell line HCC1569 × 2 (Genentech cell line repository) were used to establish xenograft models in mice for evaluation of calicheamicin ADC efficacy. HCC1569 × 2 is an *in vivo* selected variant derived from the parental HCC1569 (ATCC) for optimal growth in mice. This cell line was authenticated by short tandem repeat (STR) profiling using the Promega PowerPlex 16 System and compared with external STR profiles of cell lines to determine cell line ancestry.

To set up a WSU-DLCL2 model, tumor cells [20 million cells in 0.2-mL Hank's Balanced Salt Solution (HBSS); Hyclone] were inoculated to the flank of female C.B-17 Fox Chase SCID mice (Charles River Laboratories). For establishing HCC1569 × 2 model, tumor cells (5 million cells in 0.2 mL of HBSS supplemented with matrigel) were injected in the No. 2/3 thoracic mammary fat pad area of female C.B-17 SCID-beige mice (Charles River Laboratories). When tumors reached the desired volume (~200 mm^3), animals were divided into groups of five mice each with similar mean tumor size and received a single intravenous injection of ADCs through the tail vein (referred to as day 0). Treatment information was not blinded during tumor measurement. Tumors were measured in two dimensions (length and width) using calipers and the tumor volume was calculated using the formula: Tumor size (mm^3) = 0.5 × (length × width × width). Results were plotted as mean tumor volume ± SEM of each group over time. Animal body weights were also collected and general clinical observations were performed throughout the study. Mean (± SEM) body weight changes relative to the initial weight at day 0 were plotted overtime for each group. Mice were promptly euthanized if they displayed adverse symptoms and/or >20% weight loss.

In vivo pharmacokinetics

The *in vivo* pharmacokinetic study in mice was approved by the IACUC at Genentech, Inc. and was conducted in compliance with the regulations of the Association for Assessment and Accreditation of Laboratory Animal Care. For the mouse pharmacokinetic study, 12 female naïve C.B.17 SCID mice (6–8 weeks old) were obtained from Charles River Laboratories, Inc. Each animal received a single intravenous dose of 5 mg/kg of mAb-cal via tail vein injection. Blood samples were collected from three mice in each dosing group at each of the following timepoints: 10 minutes, 1 and 6 hours, 1, 2, 3, 7, 10, 14, and 21 days and processed for plasma. For determining the total antibody concentrations, a generic human IgG ELISA was used (33, 34). Plasma concentration–time profiles for total antibody were used to estimate pharmacokinetic parameters in mouse using a noncompartmental analysis in Phoenix 1.4 (WinNonlin pharmacokinetic software version 6.4); a naïve pooled approach was used in mouse to provide one estimate for the dose group.

In vivo stability

To determine the *in vivo* stability of ADCs, affinity capture LC/MS was performed as described previously (35). Briefly, human Ly6E extracellular domain (ECD) was biotinylated and immobilized onto streptavidin-coated paramagnetic beads (Invitrogen) in a 96-well plate, and then the ECD-bead system was used to capture anti-Ly6E disulfide conjugates by incubating with approximately 20 μL of mouse plasma samples for 1.5 hours at room temperature. The captured ADCs were then washed with HBS-EP buffer [10 mmol/L Hepes (pH 7.4), 150 mmol/L NaCl, 3.4 mmol/L ethylenediaminetetraacetic acid (EDTA), 0.005% Surfactant P20; GE Healthcare) and digested by addition of IdeS (FabRICATOR, 40 units) at 37°C for 1 hour to

remove the Fc (glycan-containing part) of the ADCs. After extensive washing of the beads with HBS-EP, water and 10% acetonitrile, the F (ab')2 portion of the ADC analytes was eluted using 30% acetonitrile in water with 1% formic acid. A KingFisher 96 magnetic particle processor (Thermo Electron) was used to mix, wash, gather, and transfer the paramagnetic beads in the above steps. A volume of 10 µL of the eluent was analyzed by LC/MS using a Triple TOF 5600 mass spectrometer (AB Sciex). Chromatographic separation of ADCs was performed on a nanoACQUITY UPLC system (Waters Corporation) equipped with a PS-DVB monolithic column (500 µm i.d. × 5 cm) (Thermo Fisher Scientific). Raw data were deconvoluted using BioPharmaView software version 1.5, and the average DAR was calculated on the basis of the peak areas of different DAR species (DAR0–DAR2).

Rat toxicology studies

To investigate the toxicity and tolerability of the aCD22-cal ADC, single-dose studies were conducted in Sprague Dawley rats. These studies were conducted in Charles River Laboratories and were conducted in accordance with USDA Animal Welfare Act (9 CFR, parts 1, 2, and 3) and as described in the Guide for the Care and Use of Laboratory Animals. Rats were dosed intravenously weekly for two doses with 4, 5, 7.5, or 10 mg/kg aCD22-cal ADC or vehicle alone, 5 or 7.5 mg/kg every 3 weeks for two doses ($n = 6$ female animals/group). Assessment of toxicity was based on body weight changes, mortality, clinical signs, and clinical and anatomic pathology. Blood collections for hematology and clinical chemistry were collected in all animals on days 5 and 15 or days 5 and 29. Additional blood collections for toxicokinetic analysis were taken on days 5 and 15 or days 5 and 29. Necropsies were performed on day 15 or 29 and tissues were routinely processed for histologic examinations.

Results

Design, synthesis, and conjugation of disulfide-activated calicheamicin derivative

We designed a calicheamicin linker drug that allows direct attachment to an engineered cysteine on an antibody via a simple unhindered disulfide linker (**Fig. 1B**). We chose to conjugate the activated disulfide calicheamicin to the attachment site, LC K149C, to provide sustained *in vivo* circulation stability. We have previously shown that disulfide linked payloads conjugated to LC K149C are stable in circulation *in vivo* and that this is due to the elevated thiol pKa of the engineered cysteine LC K149C (31, 33). The active payload would likely be generated upon internalization and proteolytic degradation of the antibody in the lysosome, followed by reduction of the cys-calicheamicin catabolite in the cytosol and subsequent Michael addition and Bergmann-type cyclization (15, 36) to yield the DNA break-inducing diradical (**Fig. 1B**).

To conjugate calicheamicin directly to the engineered cysteine thiol on the antibody, we first synthesized an activated calicheamicin containing a disulfide to 5-nitropyridine-2-thiol, a reactive leaving group (LG; Supplementary Fig. S1) to yield the linker drug, a nitroPDS-cal. We conjugated nitroPDS-cal to a LC K149C cysteine-engineered antibody targeting two different antigens, CD22 for B-cell lymphoma (37) and Ly6E, a solid tumor target expressed on breast, lung, pancreatic, kidney, ovarian, and head/neck cancers (38). The nitroPDS-cal conjugated to anti-CD22 LC K149C and anti-Ly6E LC K149C to a DAR of at least 1.7 under standard aqueous conditions with minimal organic solvent (**Fig. 2A**; Supplementary Table S1). We observed about 7% to 14% of the antibody species were conjugated to the LG, 5-nitropyridine-2-thiol, with < 1% having a free thiol remaining (**Fig. 2B**). The amount of LG was observed to be a function of the conjugation reaction pH as well as the molar excess of linker drug (Supplementary Fig. S2). Increasing the pH from 7.5 to 8.5 resulted in almost a twofold decrease in amount of conjugated 5-nitropyridine-2-thiol resulting in an increase of DAR from 1.6 to 1.8 (Supplementary Fig. S2). Furthermore, decreasing the molar excess of linker drug used from 9 × to 5 × also decreased the amount of conjugated LG a further twofold resulting also in an increase in DAR (Supplementary Table S1). Notably, there was minimal aggregation during the reaction and post purification/formulation (Supplementary Table S1). All of the conjugates prepared had less than 5% free drug and low levels of endotoxin (Supplementary Table S1).

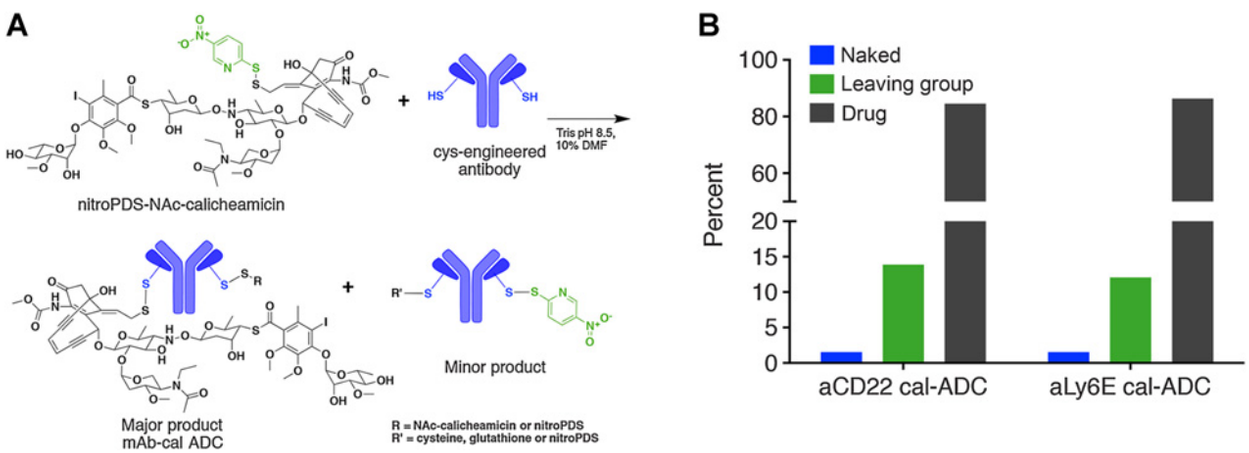

Figure 2.

Conjugation of an activated disulfide calicheamicin linker drug to a cysteine-engineered antibody. **A,** Conjugation reaction of nitroPDS-NAc-calicheamicin to an antibody engineered with a cysteine at LC K149C. The major product contains at least one conjugated drug while the other engineered cysteine maybe conjugated with drug, cysteine/glutathione or nitroPDS. The minor product consists of antibody without conjugated drug, at least one nitroPDS conjugated to the thiol while the other thiol may have cysteine, glutathione, nitroPDS or H. **B,** The percent of conjugated species were quantified by digesting the ADCs with LysC followed by LC/MS to analyze the species conjugated to the Fab fragment.

Table 1. *In vitro* cytotoxicity (IC_{50}) of calicheamicin and mAb-cal ADCs.

Cell lines	Calicheamicin[a]	aCD22-cal ADC[a]	aLy6E-cal ADC[a]
WSU-DLCL2 ($CD22^+$)	0.01	0.05	141
BJAB ($CD22^+$)	0.02	0.12	213
HCC-1569 × 2 ($Ly6E^+$)	0.04	>226	87
NCI-H1781 ($Ly6E^+$)	0.06	>226	111
Jurkat ($CD22^-$, $Ly6E^-$)	0.01	207	206

[a]Reported as nanomolar equivalents of calicheamicin.

Calicheamicin ADCs are active in cell-killing assays

We next evaluated the potency of the calicheamicin ADCs (mAb-cal) in *in vitro* cytotoxicity assays against several cell lines (**Table 1**). The aCD22 ADC had targeted activity against two different $CD22^+$ cell lines with IC_{50} values of 0.05 and 0.12 nmol/L in WSU-DLCL2 and BJAB. The aLy6E ADC also exhibited target-specific cell killing in Ly6E-expressing cell lines, HCC-1569 × 2 and NCI-1781, with IC_{50} values of 87 and 111 nmol/L. Importantly, the nontargeted ADCs had reduced activity across all of the cell lines assayed. Furthermore, in the negative control Jurkat cell line, lacking expression of both CD22 and Ly6E, both conjugates exhibited minimal potency, further supporting both the target-specific activity of the conjugates as well as the stability of these novel calicheamicin ADCs in cell culture.

Efficacy of calicheamicin ADCs in hematologic and solid tumor models

The antitumor activity of calicheamicin ADCs (mAb-cal) was evaluated in a mouse xenograft model for human non-Hodgkin lymphoma WSU-DLCL2 ($CD22^+$; ref. 37), and human $HER2^+$ breast cancer HCC-1569 × 2 ($Ly6E^+$; ref. 38). In each of the models, a control conjugate targeting an antigen not expressed in the specific tumor model was included in the study. A single dose of ADC was administered ranging from 0.3 to 10 mg/kg. The ADC was efficacious in both the liquid and solid tumor mouse xenograft models. Tumor regression was observed for doses at 3 mg/kg or higher, and the antitumor activity was durable through day 21 (**Fig. 3**). Even at a 10-fold lower dose of 0.3 mg/kg, a moderate level of activity was observed compared with vehicle or nontarget control ADC in the $CD22^+$ non-Hodgkin lymphoma model (**Fig. 3A**). In both xenograft tumor models, the ADCs were generally tolerated across the dose range administered with some dose-dependent weight loss observed in the solid tumor model (**Fig. 3C** and **D**). However, even at the highest dose of 10 mg/kg in both models, no mortality was observed.

Pharmacokinetics and *in vivo* circulation stability of calicheamicin ADC

To evaluate the circulation stability of the calicheamicin ADC (mAb-cal) conjugated to LC K149C, we measured the total antibody concentrations and attachment stability of the ADC in nontumor-bearing mice. The total antibody pharmacokinetics showed that the aLy6E ADC had a half-life of approximately 24 days with a clearance of 3.3 mL/day/kg and a total antibody exposure (AUC) of 748 (day•μg/mL) for day 0 to day 21 (**Table 2**; **Fig. 4A**). The unhindered disulfide linkage between the engineered cysteine, LC K149C, and calicheamicin appeared to be stable in circulation with 50% of the drug remaining conjugated to the antibody at the end of the 21-day study (**Fig. 4B**). Replacement of the calicheamicin on the antibody by cysteine and glutathione from the matrix was observed by mass spectrometry suggesting that disulfide exchange with circulating thiols is the mechanism for deconjugation (Supplementary Fig. S3).

Toxicity of calicheamicin ADC

The safety of the calicheamicin ADC (mAb-cal) was evaluated in rats to determine the MTD and toxicity profile. The administration of ADC weekly (qw × 2) at 10 mg/kg/dose and every 3 weeks (q3w × 2) at 7.5 mg/kg/dose were not tolerated with early euthanasia at 3 days after dose 1 of all animals (6/6) treated qw × 2 at 10 mg/kg/dose and one animal (1/6) treated q3w × 2 at 7.5 mg/kg/dose. Animals in these groups had significant body weight loss (10%; **Fig. 5**) and clinical signs consistent with general morbidity. At 5 mg/kg, both qw and q3w dosing regimens were generally well tolerated with minimal body weight loss (4%) observed (**Fig. 5**). The main pathology findings at tolerated doses were related to bone marrow hypocellularity with correlative changes in hematology parameters (decreased white blood cells and reticulocytes) and lymphoid depletion of the thymus and spleen. Minimal elevation of alkaline phosphatase was the only clinical chemistry abnormality; no histopathology correlate was present. The MTD in rats for single and repeat doses was determined to be 5.0 mg/kg with the equivalent calicheamicin dose of approximately 75 μg/kg.

Discussion

Mylotarg and Besponsa are two recently approved ADCs composed of antibodies targeting CD33 and CD22 respectively, conjugated to the potent DNA-targeting cytotoxin calicheamicin. Although these ADCs offer clinical benefit for some leukemias, they suffer from heterogeneity (including unconjugated antibody with no therapeutic benefit and species with high DAR prone to rapid clearance and toxicity), aggregation, poor stability and a narrow therapeutic index. In this study, we describe our efforts to construct a homogeneous calicheamicin ADC that is stable in circulation yet conditionally bioreversible, all while maintaining high conjugation efficiency and yield, low aggregation and efficacy with improved tolerability.

We hypothesized that we could improve the *in vivo* attachment stability of cal-ADCs by using a novel disulfide connection to directly conjugate calicheamicin to a specific site on a cysteine-engineered antibody resulting in a linkerless and traceless conjugate. This has several potential benefits over the intricate hydrazone/disulfide linker (AcButDMH) of previous cal-ADCs such as homogeneity, increased stability in circulation, and faster release in target cells. We designed and synthesized a nitroPDS cal linker drug, which was activated for conjugation through engineered cysteines on the antibody. Conjugation to LC K149C on two different antibodies, anti-CD22 and anti-Ly6E, yielded homogeneous site-specific conjugates with at least a DAR of 1.7 (**Fig. 2**). Specifically, this conjugation results in a homogenous product in contrast to the lysine conjugation chemistry utilized in Mylotarg and Besponsa that can theoretically result in over a trillion drug species as a result of a variety of DARs at potentially 40 to 70 different lysines (39, 40). A minor product of the conjugation reaction was conjugation of the nitropyridyl LG to the antibody (**Fig. 2**). For development purposes, this byproduct can be substantially reduced or even eliminated by implemention of an improved LG, such as methanethiosulfonyl (41). The most notable attribute of these linkerless calicheamicin ADCs is the remarkably low aggregation observed during the conjugation reaction, purification, and formulation (Supplementary Table S1). It has been reported for Mylotarg that significant optimization of conjugation conditions were required to mitigate

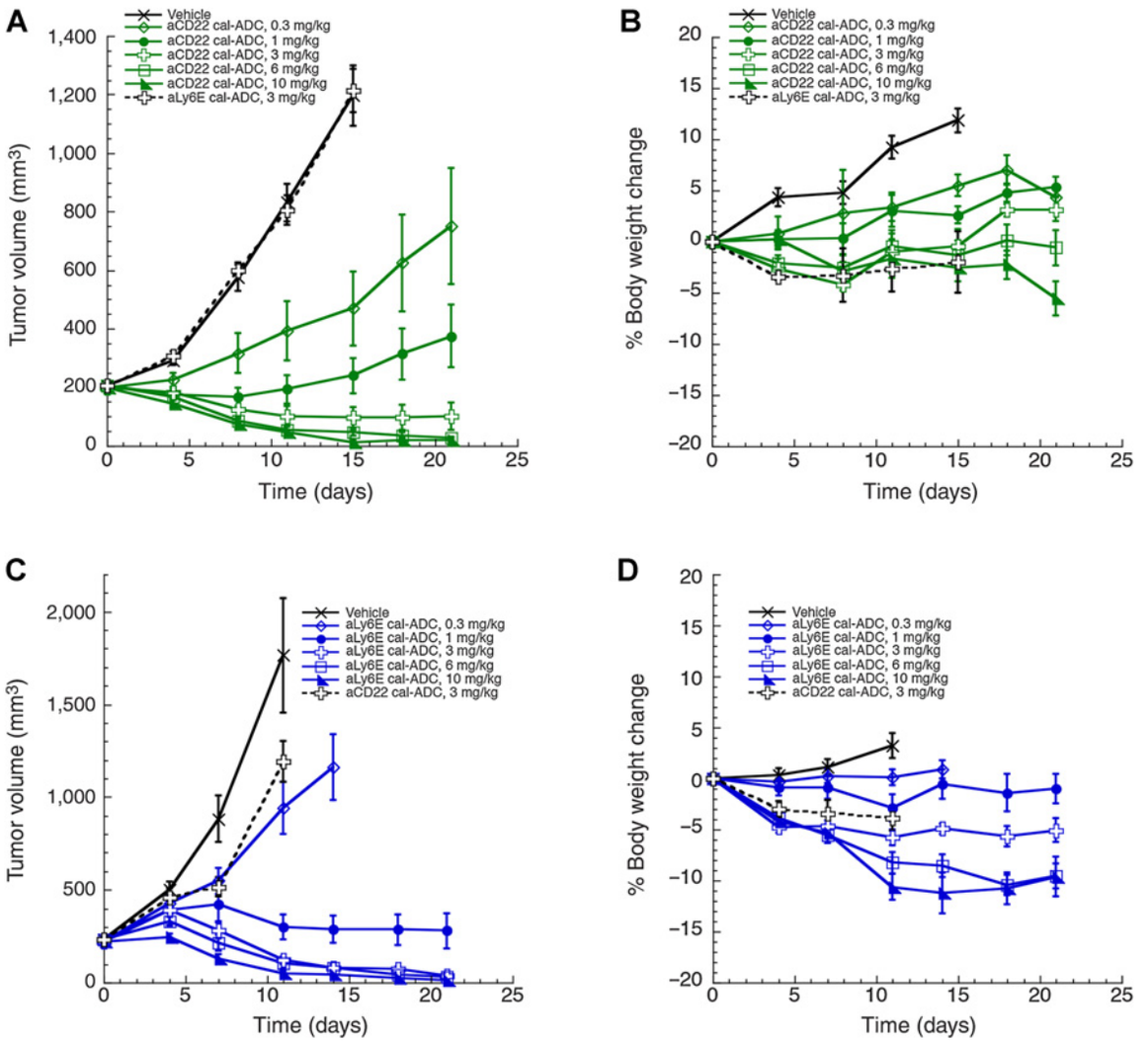

Figure 3.

In vivo efficacy and tolerability in mouse following a single intravenous dose of calicheamicin ADCs (mAb-cal). **A,** Efficacy of aCD22 LC K149C ADC evaluated in the WSU-DLCL2 xenograft model. **B,** Body weight change of the WSU-DLCL2 tumor-bearing mice dosed with aCD22 LC K149C ADC. **C,** Efficacy of aLy6E LC K149C ADC evaluated in the HCC-1569 × 2 xenograft model. **D,** Body weight change of the HCC1569 × 2 tumor-bearing mice dosed with aLy6E LC K149C ADC.

aggregation with the final approved product containing up to 50% anti-CD33 unconjugated antibody (2). The hydrophobic AcButDMH linker likely causes this aggregation. Conversely, by removing the hydrophobic linker, the linkerless calicheamicin ADCs have better biophysical properties and conjugating the drug directly to the antibody might even improve the ability of the antibody to mask the drug (42).

Table 2. Pharmacokinetic parameters of aLy6E-cal ADC in nontumor-bearing mice.

Parameters	Total antibody
Cmax (μg/mL)	105
$AUC_{0\text{-}t}$ (day•μg/mL)	748
$AUC_{0\text{-}inf}$	1,520
$T_{1/2}$ (day)	23.9
CL (mL/day/kg)	3.30

To address our hypothesis that this new calicheamicin ADC (mAb-cal) has improved *in vivo* stability, we evaluated the pharmacokinetics of the Ly6E-cal ADC in mouse. The ADC, as measured by total antibody, demonstrated a very slow clearance (< 4 mL/day/kg) and long half-life (~24 days), suggesting there was very little impact due to the conjugation of calicheamicin to the antibody (**Table 2**; **Fig. 4A**). This is supported by the similar pharmacokinetic profile exhibited by the unconjugated Ly6E antibody (43). In addition, a comparison of sparse blood samples taken during the efficacy studies revealed equivalent total antibody concentration and stability (Supplementary Fig. S4) for both Ly6E and CD22 ADCs. The stability of the disulfide between the antibody and calicheamicin was determined by monitoring the change in DAR over time. We observed approximately 50% of the drug remaining conjugated to the antibody after 21 days (**Fig. 4B**). Conversely, the reported conjugated drug half-lives were less

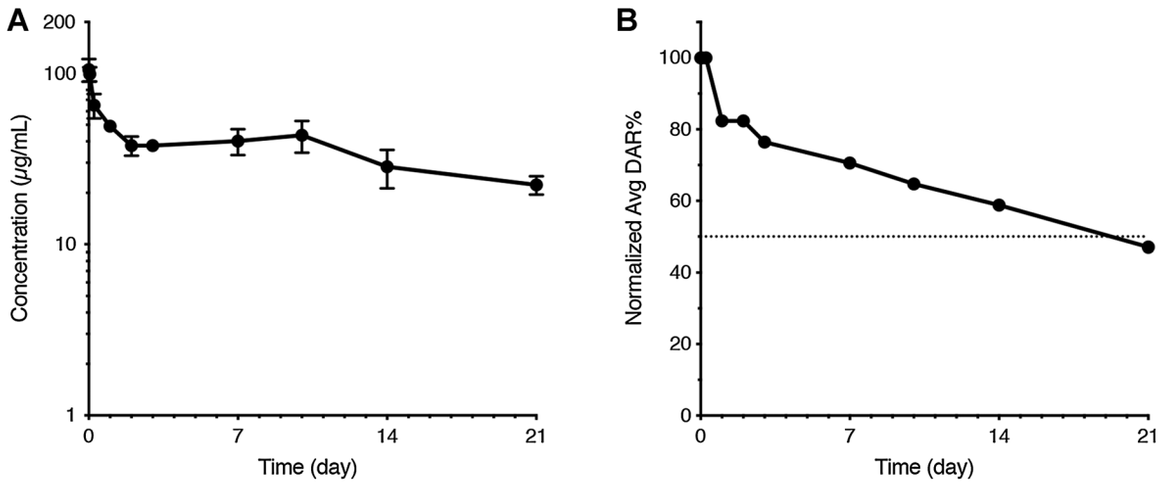

Figure 4.

In vivo pharmacokinetics and stability of calicheamicin ADC (mAb-cal) in nontumor-bearing mice. **A,** Total antibody concentration was monitored over the course of the 21 days in mice dosed with 5 mg/kg aLy6E cal-ADC using an ELISA method for generic huIgG1. **B,** Stability of aLy6E-cal ADC was monitored using LC/MS based assay to monitor the change in DAR over time.

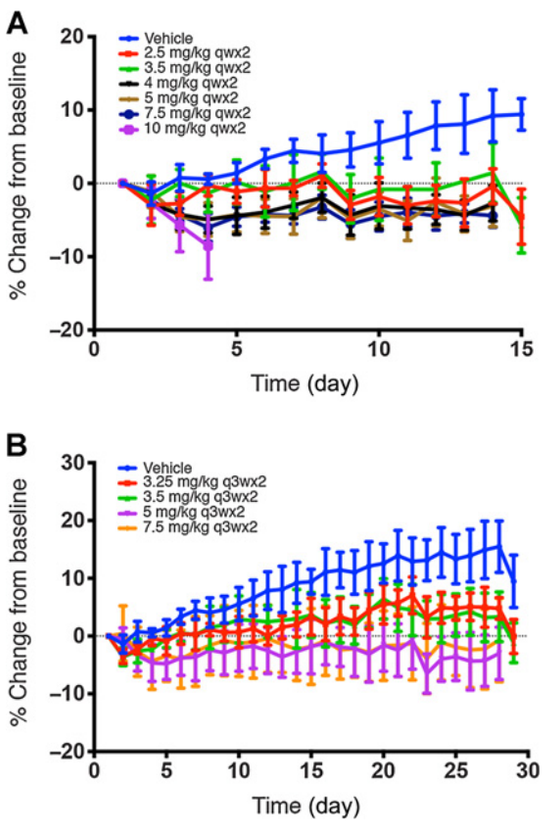

Figure 5.

Effect of linkerless calicheamicin ADC on body weight in rats. **A,** Body weight loss of rats dosed with aCD22 cal-ADC every week for two cycles. **B,** Body weight loss in rats dosed with aCD22 cal-ADC dosed every 3 weeks for two cycles.

than 2 days for both Mylotarg (47 hours) and Besponsa (29 hours) in mouse (22). Although direct comparison of the calicheamicin ADC reported here with Mylotarg and Besponsa can be difficult due to different analytic methods and endpoints, the long total antibody half-life and measurable DAR at 21 days suggests that mAb-cal is substantially more stable than either of the other cal-ADCs. The *in vivo* stability of mAb-cal containing an unhindered disulfide bond was beyond what we would have predicted on the basis of previous studies that evaluated the stability of disulfide-linked ADCs conjugated to the same antibody site (LC K149C; refs. 31–33). We previously observed that the unhindered disulfide-linked pyrrolobenzodiazepine had approximately 50% of the drug remaining on the antibody after 7 days, while the addition of a methyl group to the linker increased the amount of drug remaining to 85% at 7 days (31). With mAb-cal, we observe approximately 70% of the drug remaining conjugated to the antibody after 7 days (**Fig. 4B**). Disulfide-exchange kinetics are influenced by thiol pKa and the sterics surrounding the disulfide. It is unlikely that there is a difference in the thiol pKa of LC K149C sites across the aLy6E or aCD22 as we have previously shown that the pKa of LC K149C across these cysteine-engineered antibodies is consistent (33). One possible explanation is that the calicheamicin thiol may have an elevated thiol pKa compared with other disulfide-linked payloads we have assessed previously (31–33). Ultimately, it may be a combination of thiol pKa and sterics that afforded the significantly increased attachment stability of this calicheamicin ADC. Importantly, it is clear that this novel, linkerless connection provides a dramatic improvement in the *in vivo* stability over the AcButDMH linker used by Mylotarg and Besponsa.

Having demonstrated a significant increase in the *in vivo* circulation stability, we then assessed the activity of the calicheamicin ADCs. These ADCs are designed such that despite being quite stable, the unhindered disulfide will be rapidly bioreversible in cells, with disulfide reduction required to afford the potently bioactive molecule. By measuring the targeted cell killing activity *in vitro*, we could also draw conclusions regarding the efficiency of release as the mechanism of action for calicheamicin requires reduction to the free thiol. For the

aCD22 ADC, we observed potent, target-specific activity in both of the cell lines tested indicating that the calicheamicin thiol is released from the antibody and able to effect cell killing (**Table 1**). For the aLy6E ADC, we observed activity in the cell-based assays; however, the potency was about 1,000-fold less compared with the aCD22 ADC despite similar sensitivity to the free unconjugated parent drug. The large difference in cell potency of the ADCs is hypothesized to be related to the target biology such as differences in rate of internalization, antigen expression level, and/or efficiency of payload transport to the nucleus. More importantly, the target-specific activity of the aCD22 ADC over the 5-day continuous exposure indicating that the unhindered disulfide connection is stable in media and that the active drug is only released upon antibody-mediated internalization. *In vivo* efficacy experiments revealed that the calicheamicin ADCs (mAb-cal) are efficacious in mouse xenograft mouse models for both solid tumor ($Ly6E^+$ breast), and liquid tumor ($CD22^+$ non-Hodgkin lymphoma) indications (**Fig. 3**). Despite the differences in *in vitro* cell potency, both of the conjugates had similar *in vivo* efficacy in xenograft models with tumor regression observed through day 21 at 3 mg/kg with a single intravenous bolus dose (**Fig. 3**). Even at doses 10-fold lower (0.3 mg/kg), we were able to observe some level of efficacy across both models. Previous studies that compared the hydrazone-linked with amide-linked dimethyl disulfide cal-ADCs, concluded that for broad activity the disulfide linker alone was insufficient for activity across different indications (19, 20). However, using this stable yet bioreversible, disulfide-linked conjugate, we are able to demonstrate robust activity with mouse models for both solid and liquid tumor indications.

Having demonstrated that these novel calicheamicin ADCs are stable *in vivo* and efficacious, we next assessed the safety profile in rats. The difference in body weight loss observed is likely related to the target biology. To assess the safety profile of our cal-ADCs, we chose to evaluate our CD22 cal-ADC in rat. In comparing the single dose rat (9.8 mg/m^2) and human MTD (9.0 mg/m^2) for Mylotarg, the human MTD is relatively equivalent to the human dose of the MTD in rat, suggesting the rat is a highly relevant species for safety assessment (EMA Refusal Assessment Report for Mylotarg, 2008). For the calicheamicin ADC (mAb-cal) we observed an MTD of 5 mg/kg for both weekly and every 3 weeks dosing regimens (two doses given per schedule). We also conducted total antibody and DAR analysis on a few blood samples taken from rats dosed with CD22 cal-ADC. A limited comparison of the total antibody and DAR data for the CD22 cal-ADC in rats, in general agrees with the full assessment of Ly6E cal-ADC in mouse. The repeat dose MTD of Mylotarg in rats was reported as 7.2 mg/m^2 administered weekly for six cycles (2). Because we did not continue the study past two dose cycles we chose to compare our safety observations in rats with the reported single-dose MTD of Mylotarg. The single-dose rat MTD for Mylotarg in terms of equivalent calicheamicin drug dosed was 35 μg/kg (based on DAR 2.5) compared with the 75 μg/kg MTD determined for this calicheamicin ADC (based on DAR 1.7), suggesting a little more than twofold improvement. However, it remains unclear if the improvement in tolerability is related to the improvement in the biophysical profile of the conjugate or through increased stability of linkage between the antibody and the drug. Specifically, Mylotarg contains up to 50% unconjugated antibody with the conjugated species having an average DAR of ∼4 to 6 (2), compared with this calicheamicin ADC (mAb-cal) that is site-specific with a DAR of 1.7. Hamblett and colleagues has shown that higher DAR species are cleared faster and may lead to increased toxicity, so this could contribute to the lower MTD of Mylotarg compared with this ADC (44). Although the general target organ toxicities are similar between Mylotarg and this calicheamicin ADC (namely, affecting bone marrow), the latter was tolerated at a higher dose, suggesting an improvement in the safety of the newer ADC.

Taken together, the data we present suggest that this novel, site-specific, and linkerless calicheamicin ADC has excellent biophysical properties (uniform drug loading, low aggregation) and pharmacokinetics (high *in vivo* stability), is efficacious in both solid and liquid tumors, and has improved tolerability in rats relative to Mylotarg.

Authors' Disclosures

No disclosures were reported.

Authors' Contributions

B.S. Vollmar: Conceptualization, resources, investigation, visualization, methodology, writing–original draft, project administration, writing–review and editing. **C. Frantz:** Formal analysis, supervision, visualization, methodology, writing–original draft, writing–review and editing. **M.M. Schutten:** Formal analysis, supervision, methodology, writing–original draft, writing–review and editing. **F. Zhong:** Investigation, writing–review and editing. **G. del Rosario:** Investigation, writing–review and editing. **M.A.T. Go:** Investigation, writing–review and editing. **S.-F. Yu:** Formal analysis, supervision, methodology, writing–review and editing. **D.D. Leipold:** Formal analysis, visualization, methodology, writing–original draft, writing–review and editing. **A.V. Kamath:** Supervision, writing–review and editing. **C. Ng:** Investigation, visualization, writing–review and editing. **K. Xu:** Supervision, writing–review and editing. **J. dela Cruz-Chuh:** Investigation, visualization, writing–review and editing. **K.R. Kozak:** Supervision, writing–review and editing. **J. Chen:** Supervision, writing–review and editing. **Z. Xu:** Resources, writing–review and editing. **J. Wai:** Supervision, writing–review and editing. **P. Adhikari:** Resources, writing–review and editing. **H.K. Erickson:** Supervision, writing–review and editing. **P.S. Dragovich:** Conceptualization, supervision, project administration, writing–review and editing. **A.G. Polson:** Conceptualization, supervision, writing–review and editing. **T.H. Pillow:** Conceptualization, supervision, writing–original draft, writing–review and editing.

Acknowledgments

We thank Rebecca Rowntree, Rachana Ohri, and WuXi Biologics for support in preparation and distribution of materials described in this study.

The costs of publication of this article were defrayed in part by the payment of page charges. This article must therefore be hereby marked *advertisement* in accordance with 18 U.S.C. Section 1734 solely to indicate this fact.

Received April 29, 2020; revised September 2, 2020; accepted February 26, 2021; published first March 15, 2021.

References

1. Beck A, Goetsch L, Dumontet C, Corvaia N. Strategies and challenges for the next generation of antibody-drug conjugates. Nat Rev Drug Discov 2017;16:315–37.
2. Bross PF, Beitz J, Chen G, Chen XH, Duffy E, Kieffer L, et al. Approval summary: gemtuzumab ozogamicin in relapsed acute myeloid leukemia. Clin Cancer Res 2001;7:1490–6.
3. Petersdorf SH, Kopecky KJ, Slovak M, Willman C, Nevill T, Brandwein J, et al. A phase 3 study of gemtuzumab ozogamicin during induction and postconsolidation therapy in younger patients with acute myeloid leukemia. Blood 2013;121:4854–60.
4. Castaigne S, Pautas C, Terre C, Raffoux E, Bordessoule D, Bastie JN, et al. Effect of gemtuzumab ozogamicin on survival of adult patients with de-novo acute myeloid leukaemia (ALFA-0701): a randomised, open-label, phase 3 study. Lancet 2012;379:1508–16.
5. Amadori S, Suciu S, Selleslag D, Aversa F, Gaidano G, Musso M, et al. Gemtuzumab ozogamicin versus best supportive care in older patients with newly diagnosed acute myeloid leukemia unsuitable for intensive chemotherapy: results of the randomized phase III EORTC-GIMEMA AML-19 trial. J Clin Oncol 2016;34:972–9.

6. Norsworthy KJ, Ko CW, Lee JE, Liu J, John CS, Przepiorka D, et al. FDA approval summary: mylotarg for treatment of patients with relapsed or refractory CD33-positive acute myeloid leukemia. Oncologist 2018;23:1103–8.
7. Kantarjian HM, DeAngelo DJ, Stelljes M, Martinelli G, Liedtke M, Stock W, et al. Inotuzumab ozogamicin versus standard therapy for acute lymphoblastic leukemia. N Engl J Med 2016;375:740–53.
8. Hamann PR, Hinman LM, Hollander I, Beyer CF, Lindh D, Holcomb R, et al. Gemtuzumab ozogamicin, a potent and selective anti-CD33 antibody—calicheamicin conjugate for treatment of acute myeloid leukemia. Bioconjugate Chem 2002;13:47–58.
9. DiJoseph JF. Antibody-targeted chemotherapy with CMC-544: a CD22-targeted immunoconjugate of calicheamicin for the treatment of B-lymphoid malignancies. Blood 2004;103:1807–14.
10. Hinman LM, Hamann PR, Wallace R, Menendez AT, Durr FE, Upeslacis J. Preparation and characterization of monoclonal antibody conjugates of the calicheamicins: a novel and potent family of antitumor antibiotics. Cancer Res 1993;53:3336–42.
11. Gerber H-P, Damelin M, Sapra P. Calicheamicin antibody-drug conjugates for liquid and solid tumor indications. In: Grawunder U, Barth S, editors. Next generation antibody drug conjugates (ADCs) and immunotoxins. Cham: Springer International Publishing; 2017. p69–84.
12. Boghaert ER, Sridharan L, Armellino DC, Khandke KM, DiJoseph JF, Kunz A, et al. Antibody-targeted chemotherapy with the calicheamicin conjugate hu3S193-N-acetyl gamma calicheamicin dimethyl hydrazide targets Lewisy and eliminates Lewisy-positive human carcinoma cells and xenografts. Clin Cancer Res 2004;10:4538–49.
13. Boghaert ER, Sridharan L, Khandke KM, Armellino D, Ryan MG, Myers K, et al. The oncofetal protein, 5T4, is a suitable target for antibody-guided anti-cancer chemotherapy with calicheamicin. Int J Oncol 2008;32:221–34.
14. Leal M, Wentland J, Han X, Zhang Y, Rago B, Duriga N, et al. Preclinical development of an anti-5T4 antibody-drug conjugate: pharmacokinetics in mice, rats, and NHP and Tumor/Tissue distribution in mice. Bioconjugate Chem 2015;26:2223–32.
15. Shor B, Gerber HP, Sapra P. Preclinical and clinical development of inotuzumab-ozogamicin in hematological malignancies. Mol Immunol 2015;67:107–16.
16. Damelin M, Bankovich A, Park A, Aguilar J, Anderson W, Santaguida M, et al. Anti-EFNA4 calicheamicin conjugates effectively target triple-negative breast and ovarian tumor-initiating cells to result in sustained tumor regressions. Clin Cancer Res 2015;21:4165–73.
17. Garrido-Laguna I, Krop IE, Burris H, Hamilton EP, Braiteh FS, Weise A, et al. A phase I study of PF-06647263, a novel EFNA4-ADC, in patients with metastatic triple negative breast cancer. J Clin Oncol 35:15s, 2017(suppl; abstr 2511).
18. Hamann PR, Hinman LM, Beyer CF, Greenberger LM, Lin C, Lindh D, et al. An anti-MUC1 antibody—calicheamicin conjugate for treatment of solid tumors. choice of linker and overcoming drug resistance. Bioconjugate Chem 2005;16: 346–53.
19. Hamann PR, Hinman LM, Beyer CF, Lindh D, Upeslacis J, Flowers DA, et al. An anti-CD33 antibody—calicheamicin conjugate for treatment of acute myeloid leukemia. Choice of linker. Bioconjugate Chem 2002;13:40–6.
20. DiJoseph JF, Popplewell A, Tickle S, Ladyman H, Lawson A, Kunz A, et al. Antibody-targeted chemotherapy of B-cell lymphoma using calicheamicin conjugated to murine or humanized antibody against CD22. Cancer Immunol Immunother 2004;54:11–24.
21. Doronina SO, Toki BE, Torgov MY, Mendelsohn BA, Cerveny CG, Chace DF, et al. Development of potent monoclonal antibody auristatin conjugates for cancer therapy. Nat Biotechnol 2003;21:778–84.
22. Boghaert ER, Khandke KM, Sridharan L, Dougher M, DiJoseph JF, Kunz A, et al. Determination of pharmacokinetic values of calicheamicin-antibody conjugates in mice by plasmon resonance analysis of small (5 μL) blood samples. Cancer Chemother Pharmacol 2008;61:1027–35.
23. Advani A, Coiffier B, Czuczman MS, Dreyling M, Foran J, Gine E, et al. Safety, pharmacokinetics, and preliminary clinical activity of inotuzumab ozogamicin, a novel immunoconjugate for the treatment of B-cell non-Hodgkin's lymphoma: results of a phase I study. J Clin Oncol 2010;28:2085–93.
24. Senter PD. Potent antibody drug conjugates for cancer therapy. Curr Opin Chem Biol 2009;13:235–44.
25. Junutula JR, Raab H, Clark S, Bhakta S, Leipold DD, Weir S, et al. Site-specific conjugation of a cytotoxic drug to an antibody improves the therapeutic index. Nat Biotechnol 2008;26:925–32.
26. Bernardes GJ, Casi G, Trussel S, Hartmann I, Schwager K, Scheuermann J, et al. A traceless vascular-targeting antibody-drug conjugate for cancer therapy. Angew Chem Int Ed Engl 2012;51:941–4.
27. Gebleux R, Wulhfard S, Casi G, Neri D. Antibody format and drug release rate determine the therapeutic activity of noninternalizing antibody-drug conjugates. Mol Cancer Ther 2015;14:2606–12.
28. Shen BQ, Xu K, Liu L, Raab H, Bhakta S, Kenrick M, et al. Conjugation site modulates the *in vivo* stability and therapeutic activity of antibody-drug conjugates. Nat Biotechnol 2012;30:184–9.
29. Ohri R, Bhakta S, Fourie-O'Donohue A, Dela Cruz-Chuh J, Tsai SP, Cook R, et al. High-throughput cysteine scanning to identify stable antibody conjugation sites for maleimide- and disulfide-based linkers. Bioconjug Chem 2018;29:473–85.
30. Strop P, Liu SH, Dorywalska M, Delaria K, Dushin RG, Tran TT, et al. Location matters: site of conjugation modulates stability and pharmacokinetics of antibody drug conjugates. Chem Biol 2013;20:161–7.
31. Pillow TH, Schutten M, Yu SF, Ohri R, Sadowsky J, Poon KA, et al. Modulating therapeutic activity and toxicity of pyrrolobenzodiazepine antibody-drug conjugates with self-immolative disulfide linkers. Mol Cancer Ther 2017;16:871–8.
32. Pillow TH, Sadowsky JD, Zhang DL, Yu SF, Del Rosario G, Xu KY, et al. Decoupling stability and release in disulfide bonds with antibody-small molecule conjugates. Chem Sci 2017;8:366–70.
33. Vollmar BS, Wei B, Ohri R, Zhou J, He J, Yu SF, et al. Attachment site cysteine Thiol pKa is a key driver for site-dependent stability of THIOMAB antibody-drug conjugates. Bioconjug Chem 2017;28:2538–48.
34. Pillow TH, Tien J, Parsons-Reponte KL, Bhakta S, Li H, Staben LR, et al. Site-specific trastuzumab maytansinoid antibody-drug conjugates with improved therapeutic activity through linker and antibody engineering. J Med Chem 2014; 57:7890–9.
35. Su D, Ng C, Khosraviani M, Yu SF, Cosino E, Kaur S, et al. Custom-designed affinity capture LC-MS F(ab')2 assay for biotransformation assessment of site-specific antibody drug conjugates. Anal Chem 2016;88:11340–6.
36. Ellestad GA. Structural and conformational features relevant to the anti-tumor activity of calicheamicin gamma 1I. Chirality 2011;23:660–71.
37. Polson AG, Williams M, Gray AM, Fuji RN, Poon KA, McBride J, et al. Anti-CD22-MCC-DM1: an antibody-drug conjugate with a stable linker for the treatment of non-Hodgkin's lymphoma. Leukemia 2010;24:1566–73.
38. Asundi J, Crocker L, Tremayne J, Chang P, Sakanaka C, Tanguay J, et al. An antibody-drug conjugate directed against lymphocyte antigen 6 complex, Locus E (LY6E) provides robust tumor killing in a wide range of solid tumor malignancies. Clin Cancer Res 2015;21:3252–62.
39. Wang L, Amphlett G, Blattler WA, Lambert JM, Zhang W. Structural characterization of the maytansinoid-monoclonal antibody immunoconjugate, huN901-DM1, by mass spectrometry. Protein Sci 2005;14:2436–46.
40. Kim MT, Chen Y, Marhoul J, Jacobson F. Statistical modeling of the drug load distribution on trastuzumab emtansine (Kadcyla), a lysine-linked antibody drug conjugate. Bioconjug Chem 2014;25:1223–32.
41. Sadowsky JD, Pillow TH, Chen J, Fan F, He C, Wang Y, et al. Development of efficient chemistry to generate site-specific disulfide-linked protein- and peptide-payload conjugates: application to THIOMAB antibody-drug conjugates. Bioconjug Chem 2017;28:2086–98.
42. Su D, Kozak KR, Sadowsky J, Yu SF, Fourie-O'Donohue A, Nelson C, et al. Modulating antibody-drug conjugate payload metabolism by conjugation site and linker modification. Bioconjug Chem 2018;29:1155–67.
43. Yip V, Figueroa I, Latifi B, Masih S, Ng C, Leipold D, et al. Anti-lymphocyte antigen 6 complex, locus E-seco-cyclopropabenzindol-4-one-dimer antibody-drug conjugate that forms adduct with α1-microglobulin demonstrates slower systemic antibody clearance and reduced tumor distribution in animals. Drug Metab Dispos 2020;48:1247–56.
44. Hamblett KJ, Senter PD, Chace DF, Sun MM, Lenox J, Cerveny CG, et al. Effects of drug loading on the antitumor activity of a monoclonal antibody drug conjugate. Clin Cancer Res 2004;10:7063–70.